

RESEARCH PAPER

# FLOWERING LOCUS T-mediated thermal signalling regulates age-dependent inflorescence development in *Arabidopsis thaliana*

Pablo González-Suárez<sup>1</sup>, Catriona H. Walker<sup>1</sup>, Thomas Lock<sup>1,2</sup>, and Tom Bennett<sup>1,\*</sup>

<sup>1</sup> School of Biology, Faculty of Biological Sciences, University of Leeds, Leeds LS2 9JT, UK

<sup>2</sup> Department of Crop Genetics, John Innes Centre, Norwich Research Park, Norwich NR4 7UH, UK

\* Correspondence: [t.a.bennett@leeds.ac.uk](mailto:t.a.bennett@leeds.ac.uk)

Received 15 December 2023; Editorial decision 1 March 2024; Accepted 4 March 2024

Editor: Rainer Melzer, University College Dublin, Ireland

## Abstract

Many plants show strong heteroblastic changes in the shape and size of organs as they transition from juvenile to reproductive age. Most attention has been focused on heteroblastic development in leaves, but we wanted to understand heteroblastic changes in reproductive organ size. We therefore studied the progression of reproductive development in the model plant *Arabidopsis thaliana*, and found strong reductions in the size of flowers, fruit, seed, and internodes during development. These did not arise from correlative inhibition by older fruits, or from changes in inflorescence meristem size, but seemed to stem from changes in the size of floral organ primordia themselves. We hypothesized that environmental conditions might influence this heteroblastic pattern and found that the ambient temperature during organ initiation strongly influences organ size. We show that this temperature-dependent heteroblasty is dependent on FLOWERING LOCUS T (FT)-mediated signal integration, adding to the repertoire of developmental processes regulated by this pathway. Our results demonstrate that rising global temperatures will not affect just fertility, as is widely described, but also the size and seed number of fruits produced. However, we also show that such effects are not hard-wired, and that selective breeding for FT expression during reproductive development could mitigate such effects.

**Keywords:** Age, *Arabidopsis*, flowering, FLOWERING LOCUS T, heteroblasty, seed, temperature.

## Introduction

In angiosperms, flowering is a critical part of the plant's life cycle, one that must be tightly regulated to maximize the chances of reproductive success. To achieve this, plants have at least seven different molecular pathways that allow them to integrate exogenous and endogenous signals into the 'decision' to begin flowering (Quiroz *et al.*, 2021). While flowering time has been extensively investigated over the years,

reproductive development beyond the beginning of flowering has been much less studied. In the model plant *Arabidopsis thaliana*, flowering is characterized by the production of a variable number of inflorescences, each of which bears an inflorescence meristem (IM). While active, the IM initiates floral meristems, which hold the potential to develop into flowers and, later on, fruits (Pidkowich *et al.*, 1999; Liu *et al.*, 2009). Inflorescences,

however, have a finite life span of ~15–20 d, after which they arrest (Hensel *et al.*, 1993; Ware *et al.*, 2020). At the cellular level, this is brought about by the mitotic arrest of meristematic cells, which triggers a quiescent state of the IM (Wuest *et al.*, 2016; Wang *et al.*, 2020; Merelo *et al.*, 2022). The genetic regulation of this process is only beginning to be understood, but recent studies point towards a clear role for age (Balanzà *et al.*, 2018) and hormones (Ware *et al.*, 2020; Merelo *et al.*, 2022; Walker *et al.*, 2023). More recently, it has also been demonstrated that arrest is also environmentally controlled, with a central role for temperature, which seems to be integrated at the IM level by the floral integrator *FLOWERING LOCUST (FT)* (González-Suárez *et al.*, 2023).

Research on the end of flowering has gained traction in the past years, providing a clearer picture of the molecular processes that underlie arrest at the meristematic level. Still, little is known about other aspects of late reproductive development, despite its potential to affect seed production. Independent works have demonstrated that the timing of arrest can drastically affect inflorescence morphology and reproductive output in *A. thaliana* (Hensel *et al.*, 1993; Balanzà *et al.*, 2018; Ware *et al.*, 2020; Walker *et al.*, 2021). In other species, seed production can vary throughout flowering (Lenser *et al.*, 2018; Schmidt *et al.*, 2020), suggesting that reproductive development is influenced by the age of the plant. In fact, it is not rare for ageing to trigger changes in development during the plant's lifetime, a phenomenon named heteroblasty (Allsopp, 1967), which has received more attention during the vegetative phase, when the age of the plant at the time of organogenesis affects leaf morphology (Tsukaya *et al.*, 2000; Wang *et al.*, 2019). At the molecular level, *A. thaliana* possesses autonomously controlled mechanisms that facilitate the integration of age into different developmental programmes. Specifically, central to the ageing pathway is a regulatory hub in which two miRNAs play a leading role, miR156 and miR172. The relative balance between these miRNAs acts as a time-keeping system that regulates developmental transitions, namely from vegetative juvenile to vegetative adult and, later on, to reproduction, by affecting the transcriptional regulation of target genes (Wang, 2014; Cartolano *et al.*, 2015).

Heteroblasty has been less studied in the context of the end of flowering, although the established role for the ageing pathway during inflorescence arrest (Balanzà *et al.*, 2018) hints at a role for ageing in shaping inflorescence development more broadly. Recent results from *A. thaliana* and its close relative *Brassica nigra* suggest that fertility and seed viability change during flowering in response to ageing (Dogra and Dani, 2019), prompting a proper characterization of heteroblasty during reproductive development in members of the *Brassicaceae* family. Indeed, *A. thaliana* offers an attractive biological system to study reproductive heteroblasty, with the position of organs along the inflorescence being directly linked to the age of the plant at the time of organogenesis (Dogra and Dani, 2019). In addition to any effects of ageing on inflorescence morphology,

heteroblasty could have important implications for the quantity and quality of the offspring. Seed size is known to be affected by both parental age and the position of the source fruit within the inflorescence (House *et al.*, 2010). Furthermore, seed size is directly linked to the germination potential and seedling survival of the future generation of plants (Krannitz *et al.*, 1991; Westoby *et al.*, 1997; Manning *et al.*, 2009; House *et al.*, 2010; Krzyszton *et al.*, 2023), suggesting that reproductive heteroblasty could have direct impacts on the performance of the developing offspring.

While relationships between plant age and inflorescence development have been explored before, a proper inspection of reproductive heteroblasty is still lacking. Here, we make use of a recently proposed framework for the study of ageing during the end of flowering (Dogra and Dani, 2019) to investigate the effect of plant age on both inflorescence morphology and seed production with three main goals: (i) to characterize any signs of heteroblasty during reproductive development using *A. thaliana*; (ii) to establish what consequences said heteroblastic effects have for the next generation of plants; and (iii) to examine the control of reproductive heteroblasty by environmental signals, particularly focusing on temperature.

## Materials and methods

### Plant material

Three different plant species from the *Brassicaceae* family were used throughout the study, *Arabidopsis thaliana*, *Olimarabidopsis pumila*, and *Capsella bursa-pastoris*. Four different accessions of *A. thaliana* were used, Col-0, Ler, Kyoto, and Bâ4-1, as well as two mutants, both of which have been described before, *ft-10* (Yoo *et al.*, 2005) and *ft-1* (Koorneef *et al.*, 1991). The *ft-10* mutant is in the Col-0 background, while *ft-1* is in the Ler background.

### Plant growth

Unless otherwise specified, seeds were germinated directly on 100 ml pots filled with a 2:1 (v/v) mixture of compost (Petersfield No.2 Supreme) and perlite, and subsequently grown in controlled-environment growth cabinets (Sanyo) set at 22 °C, 16 h light:8 h dark, and ~120  $\mu\text{mol s}^{-1} \text{m}^{-2}$ . The only exception to this were the temperature experiments, where plants were grown at 20 °C until bolting, after which they were either left at 20 °C or transferred to separate cabinets set at 15 °C or 25 °C. Predatory mites (Hypoline M, Bioline Agrosociences) and nematodes (Exhibitline Sf, Bioline Agrosociences) were used as biological control for thrips and sciarid fly. For both *O. pumila* and *C. bursa-pastoris*, seeds were stratified at 5 °C in the dark for 2 d after sowing to promote germination.

### Inflorescence measurements

For internode and fruit lengths, primary inflorescences were collected once the youngest fruits were ripe. The distance from the base of the pedicel of the lowest fruit to the base of the pedicel of the next fruit was measured using digital callipers and was repeated along the inflorescence until all internode lengths were recorded. Combining all internode measurements for a single plant provided the cumulative length of the whole inflorescence. Fruit lengths were measured as the full length of the fruit, from pedicel to fruit tip.

### Plant measurements

For experiments involving measurements at the plant level, seven different traits were analysed. At bolting (i.e. the first sign of floral buds at the centre of the rosette), the number of rosette leaves was counted as a proxy for flowering time. Inflorescence duration was calculated as the number of days from bolting to inflorescence arrest (i.e. the first day that the primary inflorescence arrest stopped opening new flowers). Life span was calculated as the number of days from sowing to inflorescence arrest. Some experiments involved daily counts of the cumulative number of flowers opened in the primary inflorescence. The total number of fruits, number of fruits per inflorescence, and dry shoot weight were measured after the end of flowering was evident, namely the first day that plants stopped opening new flowers. The total number of fruits was obtained by counting all fruits produced by the plant. The number of fruits per inflorescence included only those fruits produced by the primary inflorescence. The dry shoot weight was obtained by weighing all above-ground plant material.

### Seed measurements

The number of seeds per fruit and seed area were recorded for fruits produced at different positions along the inflorescence of plants. After fruit ripening, fruits from the primary inflorescence were collected individually in 1.5 ml microcentrifuge tubes. For each plant, fruits were classified into deciles (D) depending on their relative position within the inflorescence, such that D1 corresponded to the bottom-most fruits and D10 to the top-most. One representative fruit per decile was used for seed measurements. The valves and septum were gently removed, and the seeds were imaged with a digital microscope (Keyence). Seed images were analysed using image processing software (ImageJ) to score the total number of seeds and the average seed area, which was calculated as the mean area, in  $\mu\text{m}^2$ , for all seeds within a given fruit.

### Seed germination assays

Seeds collected from different positions along the inflorescence (see ‘Seed measurements’) were harvested as soon as the fruits had visibly ripened. After at least 2 months of dry storage, they were sown onto square plates containing 8% (w/v) agarose and stratified for 2–3 d at 5 °C in the dark. Next, they were transferred to a controlled-temperature cabinet (Sanyo) set at 20 °C with continuous light ( $\sim 120 \mu\text{mol s}^{-1} \text{m}^{-2}$ ). The number of germinated seeds was then recorded after 12 h and 24 h, and every 2–3 h until 48 h.

### Meristem dissections and bud measurements

A large population of plants was grown, and plants were randomly assigned for sampling at a set number of days post-bolting. At sampling, the oldest unopened bud was assigned  $n_0$ , with the open flowers below this being  $n_{-1}$  and  $n_{-2}$ , respectively. The entire bud cluster was removed from the plant with forceps and immediately mounted into 0.5% agarose to prevent desiccation. Where fruit length is provided alongside fruit number (Fig. 1D), fruits  $n_{-1}$  and  $n_{-2}$  were left intact and allowed to ripen. Counting the number of fruits and open flowers on the inflorescence at this point provided the total fruit number. Once ripe, fruit length was measured with digital callipers as above. Buds  $n_0$  and  $n_1$  were removed from the cluster under a dissecting microscope and were mounted onto a fresh 0.5% agarose plate for imaging. The remaining buds in the cluster were then dissected and counted, until the meristem was clearly visible. The meristem was also mounted into a fresh 0.5% agarose plate for imaging. Images were collected with a Keyence VHX-700 digital microscope, using a VH-Z100R RZ $\times 100$ – $\times 1000$  real zoom lens; resulting images were analysed in ImageJ (Schneider *et al.*, 2012). Bud length was measured as the distance from the pedicel to the tip of the sepal. Meristem diameter was measured using methodology adapted from Landrein *et al.* (2015).

### Fruit removal

For fruit removal, a population of Col-0 plants was grown and those with four secondary cauline inflorescences were selected for treatment. Each of the four cauline inflorescences was assigned one of four treatments; untreated, alternate (1/2), two in three (2/3), or four in five (4/5) flowers removed. Flowers were removed when open using forceps. Fruit lengths and internode spacing were recorded with digital callipers as described above when all fruits were ripe.

### Reverse transcription–quantitative PCR

For reverse transcription–quantitative PCR (RT–qPCR), all fruits from the primary inflorescence of three randomly selected *A. thaliana* Col-0 plants were collected individually into 2 ml microcentrifuge tubes. Immediately after sampling, fruits were pooled into thirds depending on their relative position along the inflorescence, such that the first third corresponded to the bottom-most fruits and the last to the top-most. Samples were frozen in liquid nitrogen and stored at  $-80$  °C. For processing, samples were first lysed and subsequently treated with 500  $\mu\text{l}$  of Fruit-Mate (Takara Bio) prior to RNA extraction using the RNeasy Plant Mini Kit (Qiagen). The extracted RNA was treated with the TURBO DNA-free kit (Invitrogen) and used as a template for cDNA synthesis with the Transcriptor First Strand cDNA Synthesis kit (Roche). Finally, qPCR was performed using PowerUp SYBR Green Master Mix (Applied Biosystems) in a CFX Connect Real-time System (BioRad). Three qPCRs (i.e. technical replicates) were performed for each biological replicate (see ‘Experimental design and statistical analyses’) using 10 ng of cDNA and the following cycling conditions, according to the manufacturer’s guidelines: 2 min at 50 °C, 2 min at 95 °C, followed by 40 cycles of 95 °C (15 s) and 60 °C (1 min). The relative expression was obtained after normalization to the housekeeping gene *UBIQUITIN CONJUGATING ENZYME 9 (UBC9)* or *ACTIN 1 (ACT1)* using the  $2^{-\Delta\Delta\text{Ct}}$  algorithm. Primer sequences used for RT–qPCR are detailed in Supplementary Table S1.

### Experimental design and statistical analyses

Sample sizes for all experiments are indicated in the corresponding figure legends. In all cases, each replicate is obtained from an independent plant. For RT–qPCR, a biological replicate is a pool of  $\sim 15$  siliques from the same plant. Where appropriate, position along the inflorescence was calculated in deciles or quintiles by dividing the actual position of a fruit or internode (with one being the bottom-most and  $n$ , the top-most) by the total number of fruits or internodes within each inflorescence (i.e.  $n$ ). All data were analysed with the statistical software R. For sample comparisons, data were first tested for normality through visualization and with the Shapiro–Wilk test (Shapiro and Wilk, 1965) to determine the statistical tests to be used, which are indicated in the figure legends.

To test the separate and combined effects of age and temperature on inflorescence development, experimental data were fitted to a quadratic model (Equation 1), and the fitted models were used to perform an ANOVA. Additional information about the parameter estimation can be found in Supplementary Tables S2–S5.

### Equation 1. Quadratic model used to fit the experimental data.

The response variable of interest (i.e. fruit length, seed number, or seed size) was expressed as a function of the decile position ( $d$ ) and temperature ( $t$ ).  $\beta_n$  depicts the fitted coefficients (see Supplementary Tables S3 and S5).

$$f(d, t) = \beta_0 + \beta_1 d + \beta_2 d^2 + \beta_3 t + \beta_4 dt$$

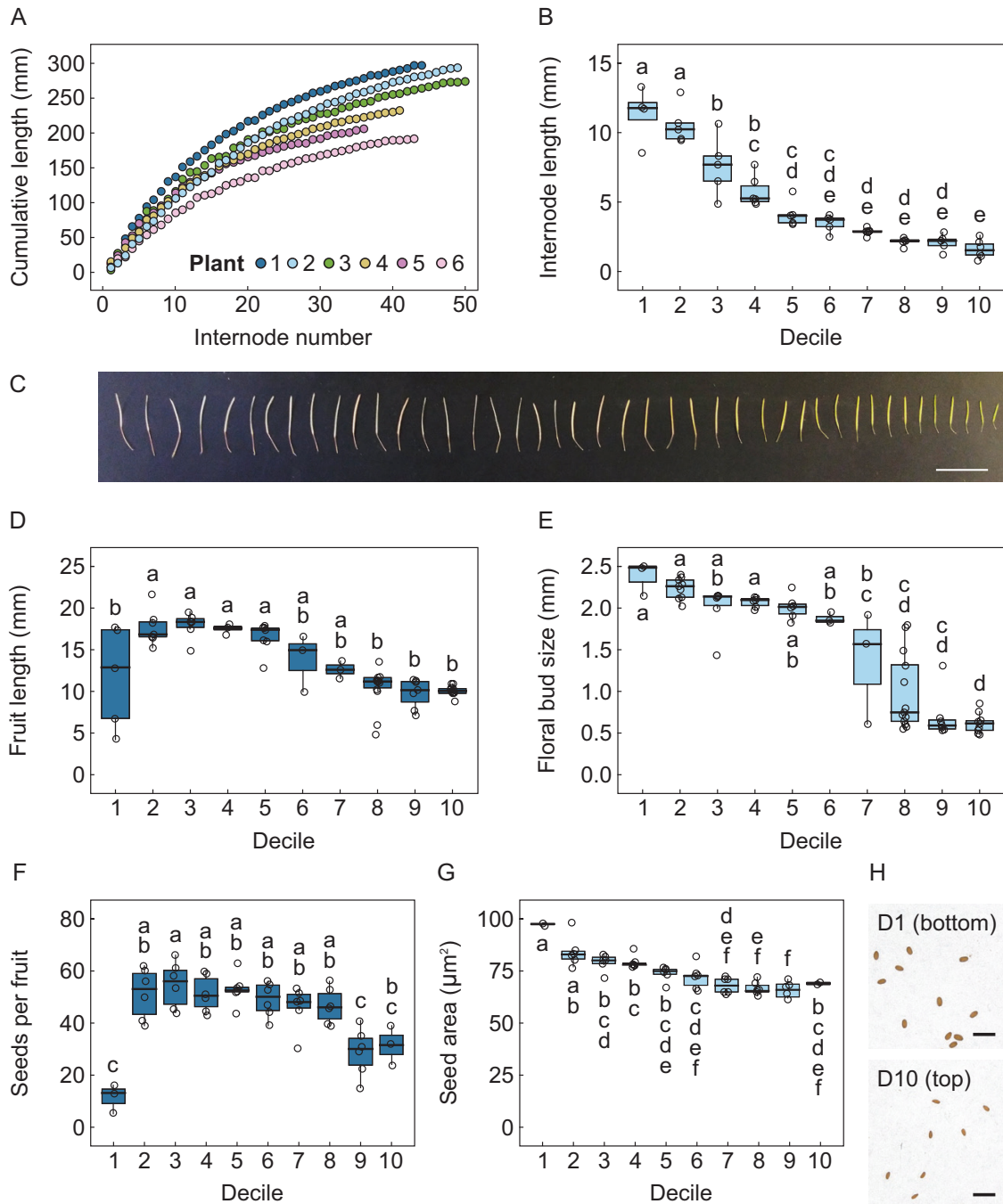


**Fig. 1.** Inflorescence development and offspring production are controlled by age. (A) Cumulative internode length along the inflorescence of individual *A. thaliana* Col-0 plants ( $n=6$ ). (B) Internode length at different positions along the inflorescence of Col-0 plants ( $n=6-7$ ). (C) Photograph of all fruits from a Col-0 inflorescence, ordered from bottom (left) to top (right). The scale bar indicates 2 cm. (D and E) Fruit length (D) and floral bud size (E) at different positions along the inflorescence of Col-0 plants ( $n=3-14$ ). (F and G) Number of seeds per fruit and average seed area in fruits from different positions along the inflorescence of Col-0 plants ( $n=6-7$ ). (H) Photographs of seeds collected from fruits located at the bottom (D1) and top (D10) of the inflorescence in Col-0 plants. The scale bar indicates 1 mm. Positions are classified into deciles such that D1 corresponds to the bottom-most fruits and D10 to the top-most. Different letters indicate statistical differences between positions (ANOVA, Tukey HSD test,  $P<0.05$ ).

## Results

Inflorescence development and offspring production are controlled by plant age

To quantify the changes in inflorescence development that occur with age, we performed detailed measurements on the morphology of wild-type *A. thaliana* Col-0. First, we measured the internode length between successive fruits along the inflorescence. The data were collected for individual plants, all of which showed the same logarithmic pattern of cumulative inflorescence length as a function of internode number (Fig. 1A). However, due to the variable number of nodes among these plants, the measurements were summarized in deciles, in line with previously published research (Dogra and Dani, 2019), where the first and tenth decile correspond to the bottom-most and upper-most positions, respectively. Unsurprisingly, we observed a clear exponential decrease in internode length with increasing internode position (Fig. 1B; Supplementary Fig. S1), consistent with the logarithmic pattern of cumulative length.

We next quantified the changes in organ size along the inflorescence with age. To do this, we grew a population of 66 plants, with each plant pre-randomized to be sampled on a certain day post-bolting. On the designated collection day, the nodal position of the oldest unopened bud was recorded ( $n_0$ ), and then the floral buds from the  $n_0$  and  $n_{+1}$  nodes were collected and measured. The immature fruits at the  $n_{-1}$  and  $n_{-2}$  position were allowed to mature fully, after which they were collected and used to record fruit length. Among this randomized sample of organs, we observed clear changes in fruit length along the inflorescence. With the exception of the first ~10 fruits, which showed high variability, fruit length was clearly greater in the base and in the middle of the inflorescence and decreased towards the top, in fruits produced at later stages in the parent's lifetime (Fig. 1C, D), consistent with previous observations on the same genotype (Dogra and Dani, 2019; Walker *et al.*, 2021). A possible explanation for this is that changes in fruit size arise from differences in earlier organ development among reproductive nodes produced at different positions and, thus, at different parental ages. Indeed, the size of floral buds decreased towards the top of the inflorescence (Fig. 1E), suggesting that the final length of the fruit may be directly linked to the size of the originating floral bud. As with fruit length, floral bud size was smaller above the eighth decile, which suggests that the small size of fruits produced at later parental ages could be caused by the smallness of the floral primordia that generated them. It is likely that a smaller floral bud would produce fewer ovules, in accordance with previous reports that ovule number decreases with age (Gomez *et al.*, 2018; Yuan and Kessler, 2019). The exception to this pattern is the bottom-most fruits, where the equivalent floral buds were actually the largest (Fig. 1D) and the ovule number is invariable (Gomez *et al.*, 2018; Yuan and Kessler, 2019), suggesting that the small size of the corresponding fruit probably arises from

low self-fertility in these flowers, for example due to a delay in the establishment of male fertility, as has been argued previously (Robson *et al.*, 2023).

Lastly, we also tested whether these developmental changes had any impact on offspring production by individually collecting fruits from different positions along the inflorescence and recording the number of seeds per fruit and the average seed area. Both parameters showed clear changes depending on their position within the inflorescence and, thus, the age of the parent at the time of organogenesis. With the exception of the bottom-most fruits, the number of seeds per fruit declined along the inflorescence (Fig. 1F) in a pattern closely resembling that of fruit length (Fig. 1D) and floral bud size (Fig. 1E). Similarly, seed area gradually decreased towards the top of the inflorescence in a manner proportional to the age of the parent (Fig. 1G, H). Taken together, these data demonstrate that the size of reproductive organs and seed, as well as the number of seeds per fruit, consistently decreases with plant age, probably due to a decline in the size of the originating floral buds, which has knock-on effects on the number of ovules per fruit.

Control of offspring production by age is widely observed in the *Brassicaceae*

A question arising from these observations was whether the control of inflorescence development and offspring production by parental age is conserved in other angiosperms. As a first approach to test this, we grew three additional accessions of *A. thaliana* in standard conditions (22 °C, 16 h light:8 h dark) and recorded both seed number and seed area for fruits placed at different positions along the inflorescence. The accessions were chosen to represent a range of inflorescence arrest phenotypes, as Kyoto and Bå4-1 are early and late arresting, respectively, and *Ler* has an inflorescence duration similar to Col-0 (Supplementary Fig. S2).

Seed number and size declined along the inflorescence in an age-dependent manner in all accessions, demonstrating that the control of offspring production by parental age is conserved across different accessions of *A. thaliana* (Fig. 2A–F). Inflorescence duration is notably shorter in Kyoto and longer in Bå4-1 (Supplementary Fig. S2); however, this did not seem to affect the heteroblastic nature of inflorescence development, suggesting that timing of the end of flowering is unlikely to be the cause of the age-dependent changes in inflorescence morphology and seed production. Based on these results, we hypothesized that the age-dependent regulation of offspring production would be conserved in the *Brassicaceae* family to which *A. thaliana* belongs. To test this, we grew two additional species, *O. pumila* and *C. bursa-pastoris*, in standard conditions (22 °C, 16 h light:8 h dark) and performed the same type of measurements. In both cases, the position of the fruit within the inflorescence clearly affected seed number and size, which exhibited patterns very similar to those of *A. thaliana* (Fig. 2G–J). The only notable difference was observed in *C.*

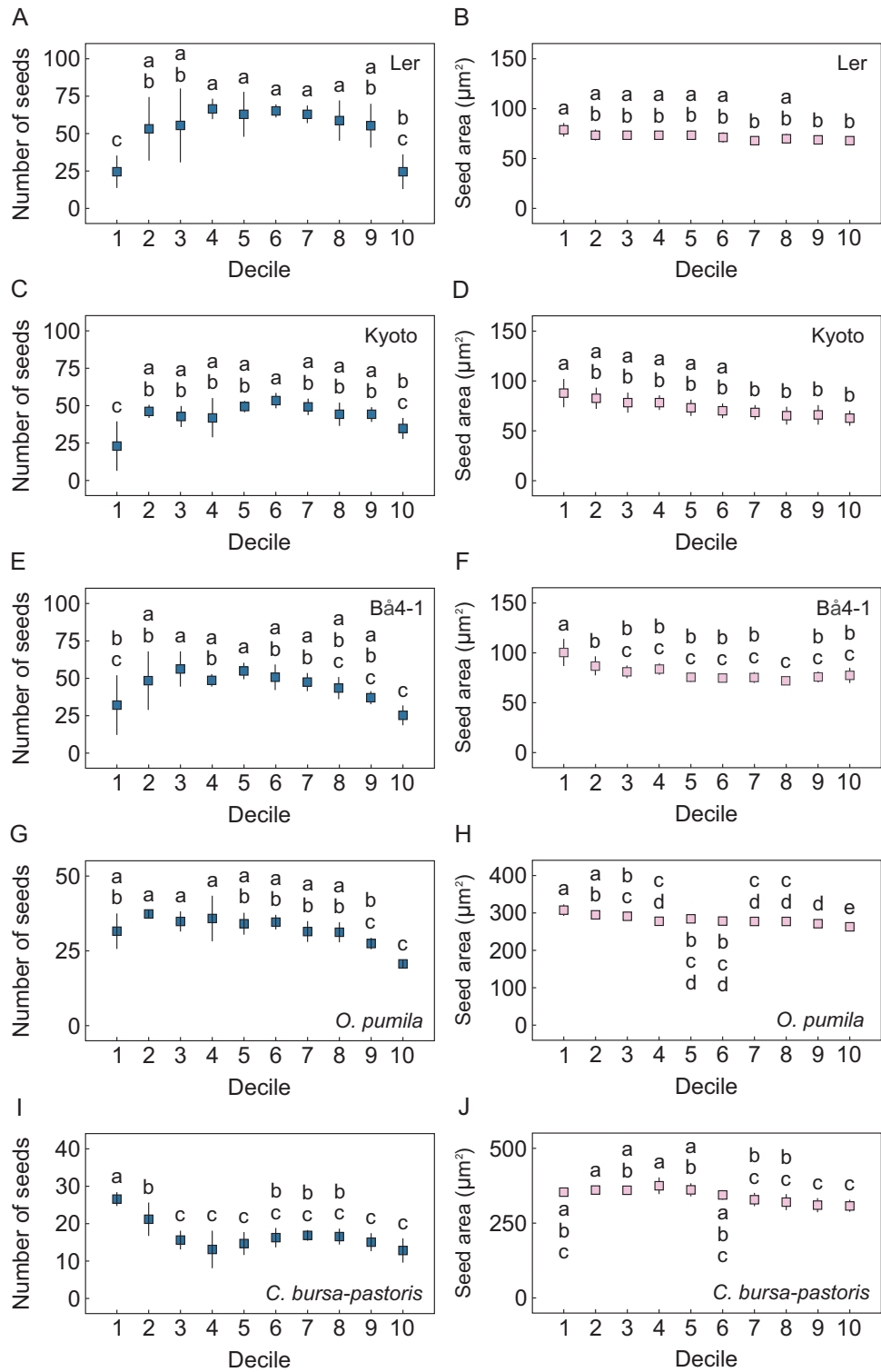


**Fig. 2.** Control of seed production by parental age is conserved in the *Brassicaceae*. Number of seeds per fruit and average seed area in fruits from different positions along the inflorescence in plants from different accessions of *Arabidopsis thaliana*, Ler (A and B), Kyoto (C and D), and Bâ4-1 (E and F), *Olimarabidopsis pumila* (G and H) and *Capsella bursa-pastoris* (I and J) ( $n=4-7$ ). Positions are classified into deciles such that D1 corresponds to the bottom-most fruits and D10 to the top-most fruits. Different letters indicate statistical differences between deciles (ANOVA, Tukey HSD test,  $P < 0.05$ ).

*bursa-pastoris*, where the bottom-most fruits showed a remarkably high fecundity (Fig. 2I), probably due to a larger allocation of resources to the first-formed fruit. However, the impact of parental age on the number and size of seeds was still evident, particularly at higher decile positions, suggesting that the control of offspring production is indeed conserved within the *Brassicaceae* family.

### Inflorescence heteroblasty has limited transgenerational impacts under optimal conditions

A key effect of inflorescence heteroblasty, which was observed for different accessions of *A. thaliana* (Figs 1G, 2B, D, F) and different species of the *Brassicaceae* (Fig. 2H, I), is the gradual decrease in seed size with greater parental age. Seed size has been previously linked to fitness potential and seedling survival (Krannitz *et al.*, 1991; Westoby *et al.*, 1997; Manning *et al.*, 2009; House *et al.*, 2010). Thus, we hypothesized that the control of seed size by parental age could affect the development of the next generation of plants and, to test this, we grew seeds produced at different positions along the inflorescence of *A. thaliana* Col-0 plants in standard conditions (22 °C, 16 h light:8 h dark) and scored multiple developmental traits related to survival, fitness, and yield.

Interestingly, seeds produced at different positions and, thus, at different parental ages, gave rise to plants with very similar characteristics (Fig. 3A–C; Supplementary Fig. S3). We found almost no differences in any of the measured traits, including the number of fruits produced (Fig. 3B) and the final shoot biomass (Fig. 3C). With minor exceptions, flowering time, inflorescence duration, and, ultimately, life span were not significantly affected by the position of the source fruit within the inflorescence (Supplementary Fig. S3), suggesting that the life expectancy of the offspring is not affected by the age of the mother plant at seed set. Altogether, these results suggest that parental age has a very limited impact on the development of the future generation of plants, at least under optimal conditions. As seed size affects germination (Murali, 1997; van Mølken *et al.*, 2005), and given that seed size is definitely controlled by age in *A. thaliana* (Figs 1G, 2), we hypothesized that parental age could affect the development of offspring in a more immediate way by controlling their germination potential. To test this, we performed a germination assay using seeds collected from different positions along *Ler* inflorescences. While there were no differences in the germination potential of seeds, all of which eventually germinated after 48–72 h, we noted that seeds from the top of the inflorescence had a noticeably slower germination rate (Fig. 3D, E). As these come from fruits that are produced when the mother plant is the oldest, these results indicate that age impacts not only the morphology of inflorescences and seeds but also the early development of the next generation of plants. In light of these findings, we decided to focus on identifying potential causes and regulators of the age-dependent control of inflorescence development.

Control of inflorescence development by age is not affected by older fruits, developmental rate, or inflorescence meristem size

Fruits are a well-established source of correlative inhibition in the shoot system (Bangerth, 1989), and we have previously shown how *A. thaliana* fruits exert dominance to bring about inflorescence arrest (Ware *et al.*, 2020). We therefore hypothesized that the age-related change in inflorescence development could be the result of earlier fruit inhibiting the development of later formed reproductive tissues. To test this, we used a population of plants that each had four secondary cauline inflorescences, allowing us to perform four differential treatments between the inflorescences of the same plants. The treatments we performed were to remove either no fruit (untreated), every second fruit (1/2), two out of every three fruits (2/3), or four out of every five fruits (4/5), thus leaving either 100, 50, 33, or 20% of fruits evenly spaced along the inflorescence. After all inflorescences had arrested, we recorded internode and fruit lengths along the inflorescences. We observed that fruit removal treatments had no effect on internode length, with the same reduction in spacing towards the top of the inflorescence occurring in all treatments (Fig. 4A). Similarly, while fruit removal treatments had a significant effect on fruit length, the age-dependent changes were largely unaffected, with similar heteroblastic patterns occurring in all treatments (Fig. 4B). In light of these data, we concluded that feedback from older fruit is probably not the main driver of inflorescence heteroblasty in *A. thaliana*, although its influence cannot be completely ruled out, particularly in controlling seed number and size.

Across multiple experiments, we found that, under our growth conditions, *A. thaliana* inflorescences open flowers at a constant rate between bolting and inflorescence arrest (Fig. 4C), giving no indication of an acceleration in developmental rate during the inflorescence's lifetime. However, it is possible that the rate of flower opening is disconnected from the rate of initiation of floral primordia. To resolve this, we dissected primary inflorescences each day post-bolting in a separate experiment to monitor the total number of reproductive nodes (floral primordia, floral buds, flowers, and fruits). In this new experiment, we found that the number of both total nodes and opened flowers steadily increase at a constant rate of  $\sim 2.5 \text{ d}^{-1}$  until inflorescence arrest (Fig. 4D). Ultimately, our data do not indicate any significant change in developmental rate during inflorescence development, and thus suggest that changes in developmental rate are not a likely cause of inflorescence heteroblasty.

We next hypothesized that the heteroblastic inflorescence development may be caused by the decrease in the size of the IM which has been described to occur at the end of flowering (Wang *et al.*, 2020; Merelo *et al.*, 2022; Walker *et al.*, 2023) (Fig. 4E). To further explore this idea, we tracked changes in meristem size every day post-bolting and recorded the final fruit and internode lengths across the inflorescence. At first

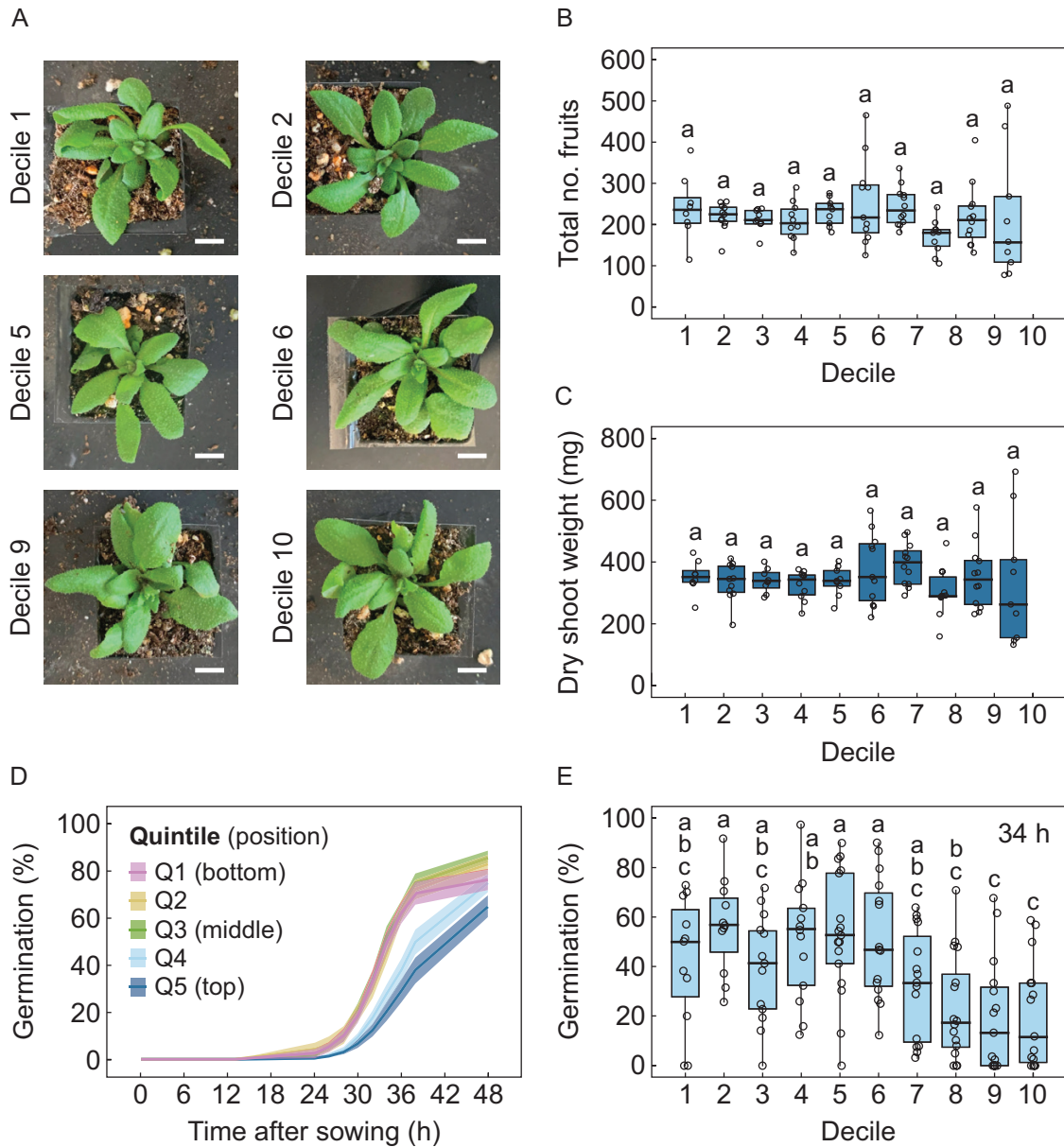


**Fig. 3.** Transgenerational effects of parental age are limited to early development. (A) Photographs of plants grown from seed produced at different positions along the inflorescence of *A. thaliana* Col-0 at flowering. The scale bar indicates 1 cm. (B and C) Total number of fruits (B) and final shoot biomass (C) in plants grown from seeds belonging to different positions along the inflorescence of *A. thaliana* Col-0 ( $n=9-12$ ). (D) Seed germination rates of *Ler* seeds from different positions along the inflorescence ( $n=4$ ). (E) Proportion of germinated *Ler* seeds from different positions along the inflorescence 34 h after sowing ( $n=4$ ). Positions are classified into deciles (D) or quintiles (Q) such that D1 and Q1 corresponds to the bottom-most fruits and D10 and Q5 to the top-most fruits. Different letters indicate statistical differences between offspring groups (ANOVA, Tukey HSD test,  $P<0.05$ ).

glance, the changes in IM size that take place during flowering seemed to be echoed by the changes in fruit length, both of which decrease at similar time points and at comparable rates (Supplementary Fig. S4A, B), suggesting that inflorescence heteroblasty may indeed be caused by a reduction in IM size. However, when both datasets were re-plotted as a function of the cumulative number of reproductive nodes, it became clear that the decline in fruit length occurs too early to be caused by the change in IM size (Fig. 4F). The same was true for the

decline in internode length, which is seen in older parts of the inflorescence, in nodes produced days prior to the decrease in IM size (Supplementary Fig. S4C). If the activity of a smaller IM caused inflorescence heteroblasty, the first fruits and internodes to show a decline in length should occur after node 40 (Fig. 4F). However, the decrease in fruit (Fig. 4F) and internode (Supplementary Fig. S4C) length occurs much earlier, suggesting that, rather than changes in IM size causing changes in fruit and internode size, all three parameters are



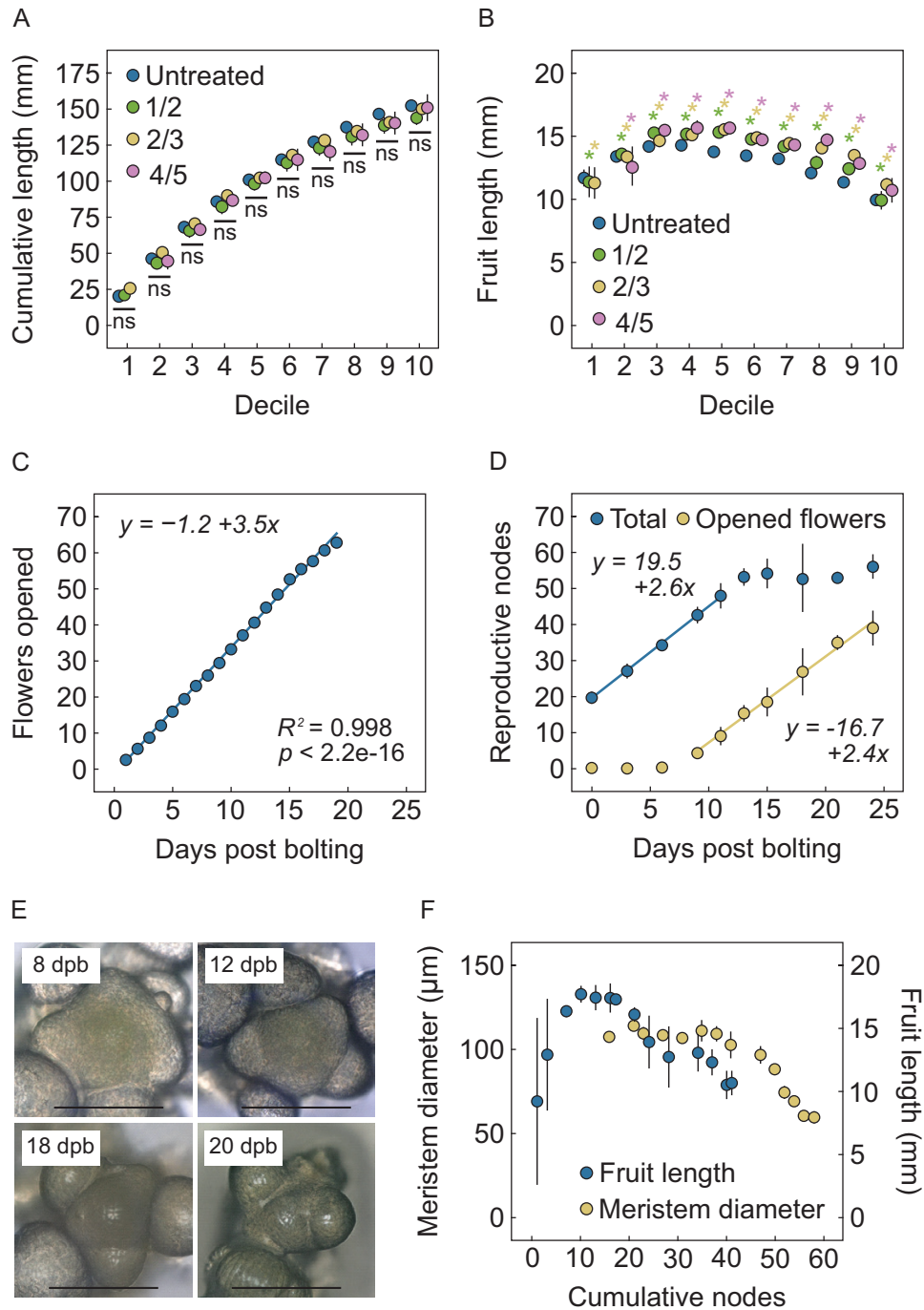


**Fig. 4.** Age-dependent control of inflorescence development is not affected by feedback from the fruits, a slower developmental rate, or a decrease in meristem size. (A and B) Cumulative internode length (A) and fruit length (B) at different positions along the inflorescence in plants with no fruit removed (untreated) or in which every second fruit (1/2), two out of every three fruits (2/3), or four out of every five fruits (4/5) were removed ( $n=6$ ). Positions are classified into deciles such that D1 corresponds to the bottom-most fruits and D10 to the top-most fruits. Asterisks indicate statistical differences against the untreated control for each decile; ns=not significant. (C) Number of opened flowers recorded at different time points during flowering ( $n=24$ ). The smooth line indicates the best fit for a simple linear model. Parameter estimations, adjusted  $R^2$ , and  $P$ -value are indicated. (D) Total number of reproductive nodes and cumulative number of opened flowers recorded at different points during flowering ( $n=3-8$ ). Smooth lines indicate the best fit for a simple linear model (blue:  $R^2=0.99$ ,  $P$ -value= $7.8e-6$ ; yellow:  $R^2=0.99$ ,  $P$ -value= $1.6e-6$ ). Parameter estimations are indicated in the graph. (E) Photographs of the inflorescence meristem from the primary inflorescence of a Col-0 plant at different time points during flowering. The scale bar represents 100  $\mu\text{m}$ ; dpb, days post-bolting. (F) Diameter of the inflorescence meristem and fruit length measured at different time points during flowering, plotted as a function of the number of reproductive nodes that had been produced at each time ( $n=3-8$ ).

likely to be responding to the same external stimulus at the same time.

### Thermal exposure during flowering affects the age-dependent control of inflorescence development

We therefore speculated that external cues may regulate the age-dependent control of inflorescence development. Recently, we have shown that temperature has a key role in the regulation of late reproductive development in *A. thaliana* (González-Suárez *et al.*, 2023). Thus, we hypothesized that the temperature experienced by plants during flowering would impact the control of inflorescence development by plant age. To test this, we grew Col-0 plants at 20 °C (16 h light:8 h dark) until visible bolting, after which we transferred subsets of plants to two different temperatures, 15 °C and 25 °C. After end of flowering and fruit ripening, we collected individual fruits from different positions along the inflorescence and recorded fruit length, seed number per fruit, and seed size. In these experiments, both fruit length and the number of seeds per fruit were higher at the bottom and in the middle of the inflorescence, except in the first decile, as previously described (Fig. 1D, F), at all temperatures (Fig. 5A, B). In accordance, the effect of the decile position on these parameters was statistically significant at each temperature (Supplementary Table S2). As also previously observed, seed area gradually declined towards the top of inflorescences (Fig. 5C), which was also statistically significant for each temperature tested (Supplementary Table S2). For all three traits, temperature during flowering had clear effects on reproductive development and heteroblasty, and also showed an interaction with parental age. Firstly, increasing temperature reduced the size of fruits, the number of seed per fruit, and the seed area in each decile of the inflorescence (Fig. 5A–C). Secondly, at higher temperatures, the effect of parental age on heteroblastic fruit length and seed number was subtler (Fig. 5A, B), whereas the opposite was true for seed area (Fig. 5C), as evidenced by the significant effect of the interaction between decile position and temperature (Supplementary Table S2). These results indicate a clear interaction between temperature and parental age, as the extent of age-dependent effects was influenced by the temperature experienced by the parent. Although trade-offs between seed number and size are known (Manning *et al.*, 2009; Dogra and Dani, 2019), our findings suggest that these traits can also be controlled independently, leading to distinct responses to environmental inputs such as temperature. Furthermore, the data presented here demonstrate that parental age and temperature interact with one another to control inflorescence development and offspring production.

A question raised by these data is at what point during development does temperature control operate. To answer this, we performed a transfer experiment where we grew a population of plants at 20 °C (16 h light:8 h dark) and transferred subsets of this population to 25 °C at 0, 4, 8, 12, or 16 d post-bolting. After all fruits ripened, we assessed inflorescence

heteroblasty for all transfer groups by measuring fruit length, which is a good proxy for the number of seeds per fruit ( $r=0.7$ ,  $R^2=0.5$ , Supplementary Fig. S5). Transferring plants to 25 °C immediately after bolting caused a reduction in fruit lengths for all positions along the inflorescence (Supplementary Fig. S6), as previously described. There were almost no differences between plants transferred after 0 d and 4 d of flowering, neither of which had opened flowers at the time of transfer (Supplementary Fig. S6), suggesting that temperature experienced by unopened floral primordia does not affect their subsequent development as fruits. However, transfer groups which had open flowers and young fruits when they were transferred showed an effect on fruit lengths for the deciles corresponding to these open flowers (i.e. the third, fourth, and sixth decile for plants transferred after 8, 12, and 16 d, respectively), and in all subsequent deciles. Based on this, we concluded that temperature controls fruit development by acting specifically during early flower stages, with very little effect of the prior temperature experienced during the initiation of floral primordia.

### Inflorescence heteroblasty is regulated by *FLOWERING LOCUS T*

Previously, temperature experienced by the mother plant has been shown to affect seed dormancy through a process partially mediated by *FT* (Chen *et al.*, 2014), an integrator of environmental signals during flowering (González-Suárez *et al.*, 2023). Thus, we hypothesized that *FT* could also regulate the control of offspring production by plant age and/or its interaction with temperature. To test this, we included *ft-10* mutants as part of the previous experiment, where they were grown at 20 °C (16 h light:8 h dark) until bolting and subsequently transferred to either 25 °C or 15 °C, with control plants left at 20 °C. After the end of flowering, we collected ripened fruits and measured fruit length, seed number, and seed area. Similar to wild-type plants, age impacted fruit length and seed number of *ft-10* at all temperatures (Fig. 5D, E), with warmer temperatures negatively affecting the number of seeds per fruit for all decile positions (Fig. 5E; Supplementary Table S2). However, although the effect of age on development was statistically significant, *ft-10* mutants had much less obvious heteroblasty, showing a smaller decline in fruit length, seed number, and seed area across the inflorescence (Fig. 5D–F). Additionally, while warmer temperatures diminished the effect of age on inflorescence development and offspring production in the wild type (Fig. 5A), this was less notable for *ft-10*, where the interaction between age and temperature was only marginally significant (Supplementary Table S2). These data seemed to suggest that *FT* is necessary for the interplay between plant age and temperature experience. This was even clearer when considering seed area. While in the *ft-10* mutant the effect of age and temperature on seed area was marginally significant (Supplementary Table S2), the extent of age-related changes in seed area was much less obvious compared with the wild

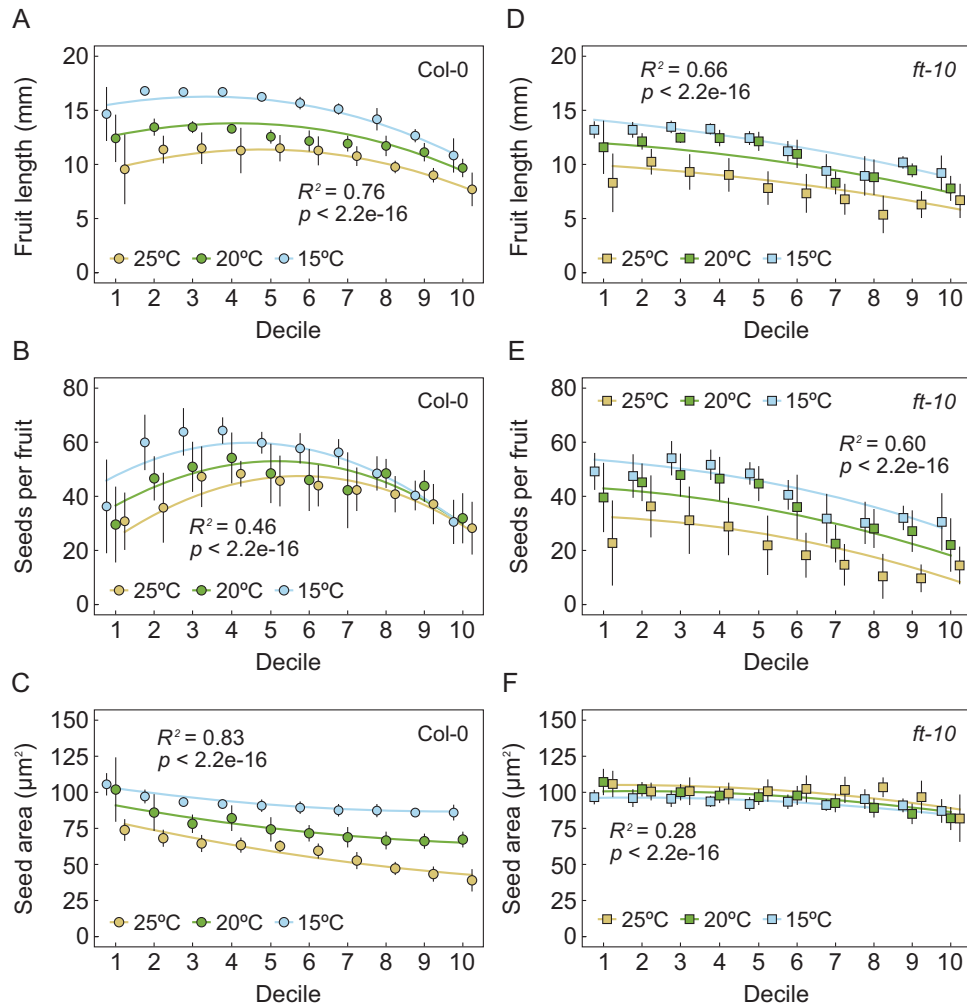


**Fig. 5.** Control of seed production by parental age is regulated by temperature in an FT-dependent manner. (A–C) Fruit length (A), number of seeds per fruit (B), and average seed area (C) in fruits from different positions along the inflorescence of Col-0 plants flowered at 15, 20, or 25 °C ( $n=3-5$ ). (D–F) Fruit length (D), number of seeds per fruit (E), and average seed area (F) in fruits from different positions along the inflorescence of *ft-10* mutants flowered at 15, 20, or 25 °C ( $n=3-4$ ). Positions are classified into deciles such that D1 corresponds to the bottom-most fruits and D10 to the top-most fruits. Points represent means, and error bars represent the SD. Coloured smooth lines indicate the best fit for a quadratic model with the formula indicated in Equation 1 (see [Supplementary Tables S2 and S3](#)). Adjusted  $R^2$  and  $P$ -values for each model are indicated in each panel.

type (Fig. 5F). Furthermore, there was almost no difference in seed area due to temperature treatment (Fig. 5F). Altogether, our results point towards a role for *FT* in linking plant age and temperature during flowering, ultimately allowing plants to precisely modulate inflorescence and seed development in response to both internal and external cues.

To validate the involvement of *FT* in these processes, and to discard any other background-specific causes for the *ft-10* phenotype, we repeated a simplified version of the experiment using the *ft-1* mutant, which is in the *Ler* background. We grew both mutant and wild-type plants at 20 °C (16 h light:8 h dark) until bolting, after which we transferred a subset of them to 25 °C. We then measured fruit and internode lengths along the inflorescence after all inflorescences arrested and fruits were visibly ripened. *Ler* showed signs of inflorescence heteroblasty

(Fig. 6A, B; [Supplementary Table S4](#)) similar to those of Col-0, in accordance with previous assessments of seed traits in the same genotype (Fig. 2A, B). At warmer temperatures, *Ler* plants also showed a statistically significant reduced effect of age on fruit length, which was not observed in *ft-1* mutants (Fig. 6A; [Supplementary Table S4](#)), further supporting the idea that functional *FT* is necessary for the appropriate integration of temperature and age signals during seed set. Internode length decreased with age in both genotypes and at both temperatures, but showed a stronger decline with age at warmer temperatures in the wild type, which was not observed in *ft-1* (Fig. 6B; [Supplementary Table S4](#)), suggesting that *FT* also affects inflorescence stem morphology.

We had noted that heteroblastic effects during inflorescence development have implications for the germination potential

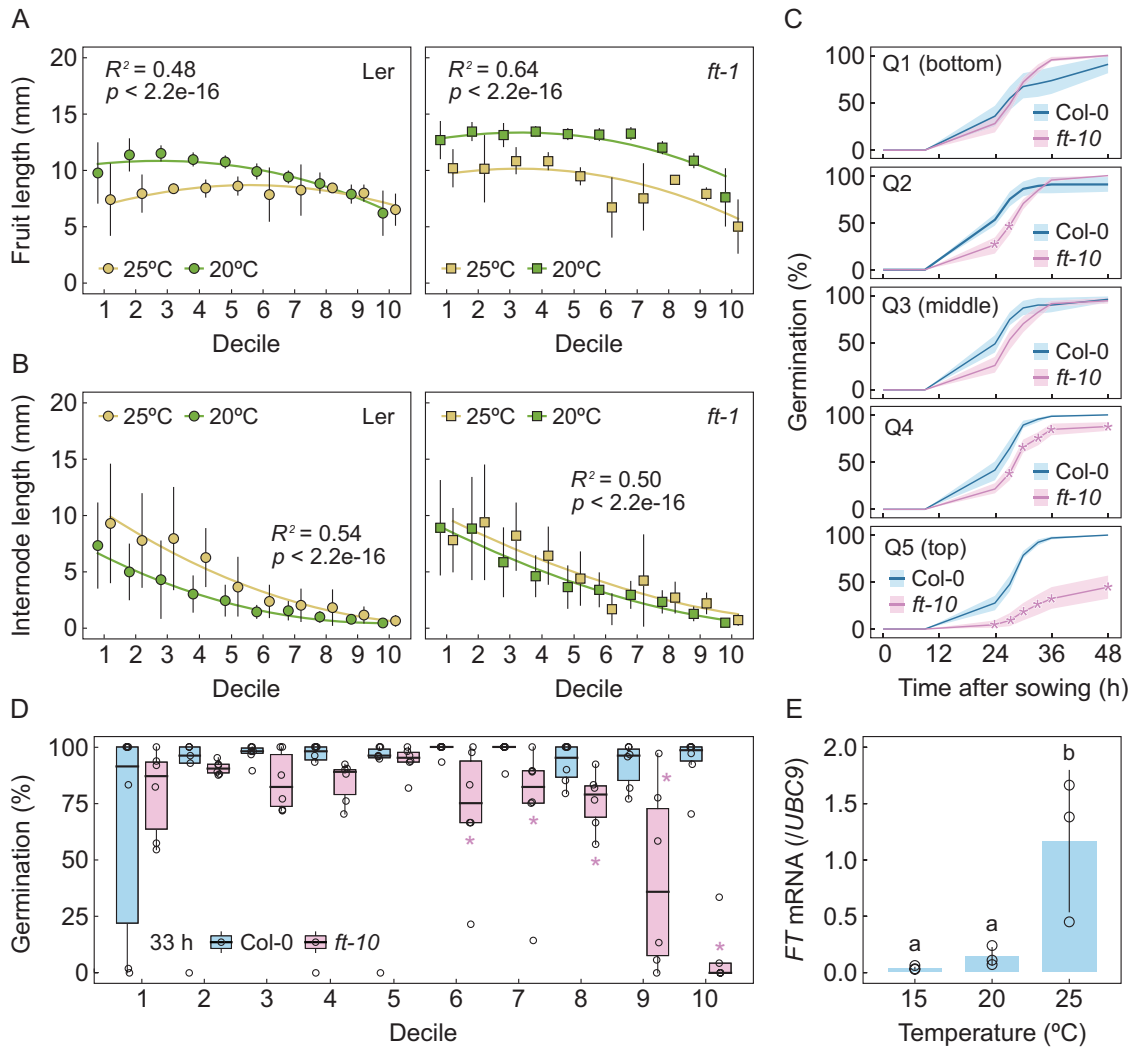


**Fig. 6.** A mechanism based on the temperature-dependent transcriptional regulation of FT probably controls seed traits. (A and B) Fruit length (A) and internode length (B) at different positions along the inflorescence of Col-0 (left) or *ft-1* (right) plants flowered at 20 °C or 25 °C ( $n=4$ ). Coloured smooth lines indicate the best fit for a quadratic model with the formula indicated in Equation 1 (see [Supplementary Tables S4 and S5](#)). (C) Seed germination rates of Col-0 and *ft-10* seeds from different positions along the inflorescence ( $n=6$ ). Asterisks indicate statistical differences from the wild type within each time point (ANOVA, Tukey HSD test,  $P<0.05$ ). (D) Proportion of germinated seeds from different positions along the inflorescence 33 h after sowing ( $n=6$ ). Asterisks indicate statistical differences between genotypes within each decile (Wilcoxon test,  $P<0.05$ ). (E) *FT* expression in fruits from the top third of arrested inflorescences exposed to 15, 20, or 25 °C ( $n=3$ ). Transcript levels are normalized to *UBC9* and then to the maximum *FT* level. Error bars indicate the SD. Different letters indicate statistical differences between temperatures (ANOVA, Tukey HSD test,  $P<0.05$ ). Positions are classified into deciles or quintiles such that Q1 and D1 corresponds to the bottom-most fruits and Q5 and D10 to the top-most fruits.

of seeds (Fig. 3D, E), and it has previously been shown that *FT* controls seed dormancy (Chen *et al.*, 2014). Thus, we questioned whether the lack of heteroblasty that we found in the seeds of *ft* mutants (Fig. 5F) would have implications for their germination. To test this, we performed a germination assay using seeds collected from different positions along Col-0 and *ft-10* inflorescences. Interestingly, while the oldest seeds did not show differences in their germination rate or potential between the wild type and *ft-10*, younger seeds within the inflorescence exhibited a slower and poorer germination in the *ft-10* mutant (Fig. 6C, D). This was striking considering that these seeds showed virtually no differences in seed area

(Fig. 5F), suggesting that seed size and germination may be targeted by different regulatory mechanisms during late reproductive development. Ultimately, our results also indicate that *FT* signalling is implicated in the combined regulation of seed traits by age and temperature, including seed number and area, and seed germination.

Previously, temperature during flowering has been shown to affect *FT* expression in leaves and fruits (Chen *et al.*, 2014; González-Suárez *et al.*, 2023). Thus, we hypothesized that a mechanism based on the transcriptional regulation of *FT* could underlie the control of inflorescence heteroblasty. To test this, we measured *FT* expression in whole, undissected fruits from

different positions along the inflorescence of plants that flowered at either 15, 20, or 25 °C. We were unable to detect *FT* mRNA in fully developed fruits from the bottom and middle of the inflorescence, suggesting that *FT* expression is lost in mature seeds/fruits. On the contrary, we were able to quantify *FT* transcript levels in the top-most, developing fruits, where *FT* expression was clearly up-regulated at warmer temperatures (Fig. 6E; Supplementary Fig. S7). Temperature-dependent regulation of *FT* transcription has been demonstrated for various plant tissues (Blázquez *et al.*, 2003; Chen *et al.*, 2014; Thines *et al.*, 2014), and the data presented here demonstrate that *FT* expression in the fruits is also controlled by age. Based on these findings, it is tempting to speculate that plant age and temperature interact at the level of *FT* transcription in fruits, to modulate seed production.

## Discussion

Here, we have shown that age controls inflorescence development by affecting the size of multiple reproductive organs (Fig. 1), and that this is conserved within the *Brassicaceae* family (Fig. 2). Fruits produced by older parents contain fewer seeds (Fig. 1F), in accordance with previous reports (Dogra and Dani, 2019), and these later produced seeds are smaller (Fig. 1G, H). While there are known trade-offs between seed size and number (Manning *et al.*, 2009; Dogra and Dani, 2019), our data suggest that these effects are probably bypassed in older parents. We observed age-dependent effects even in fruits produced days prior to arrest and the onset of senescence (Wang *et al.*, 2020), suggesting that these are not likely causes of inflorescence heteroblasty. Instead, it is likely that molecular time-keeping mechanisms acting throughout the whole inflorescence life span control this process. The miR156/miR172-regulated ageing pathway, which is known to affect the timing of arrest (Balanzà *et al.*, 2018), would be an interesting candidate for this, and future research would benefit from a proper assessment of its involvement in reproductive heteroblasty. We have also demonstrated that parental age has very limited effects on the development of the future generation of plants under optimal conditions (Fig. 3), which is in accordance with similar work on other plant species such as pine tree (Pardos *et al.*, 2022) and duckweed (Barks and Laird, 2015). It is possible, however, that the development of the offspring could be affected in suboptimal environmental scenarios, and future research would benefit from addressing this question. Indeed, a recent report demonstrates that parental age impacts stress tolerance in the aquatic plant *Lemna minor* (Chmilar and Laird, 2023). In addition, we have shown that the age of the parent impacts the germination of the offspring seed, even in optimal conditions (Fig. 3D, E). Previously, it has been proposed that the decline in fertility in fruits produced by older parents is associated with an increase in both seed size and seed germination potential (Dogra and Dani, 2019), but our results

contradict this model. Smaller seeds from the top of the inflorescence germinate more slowly, in agreement with a recent study that reports a higher level of dormancy in small seeds (Krzyszton *et al.*, 2023).

As both seed size and seed dormancy are key factors influencing seedling vigour (Murali, 1997; van Mólken *et al.*, 2005), it is expected that their response to plant age would be tightly controlled at the genetic and environmental levels, although the nature of these remains unknown. Our data suggest that endogenous signals that are known to affect end of flowering, such as feedback from the fruits (Hensel *et al.*, 1993; Wuest *et al.*, 2016; Walker *et al.*, 2021) or the decline in IM size that takes place during flowering (Wang *et al.*, 2020; Merelo *et al.*, 2022; Walker *et al.*, 2023), do not affect this process, nor are they caused by a shift in the rate of organogenesis (Fig. 4). The observed heteroblastic effects could instead arise from a gradual decline in the size of floral meristems with plant age, which may ultimately translate into the smaller floral bud size that we observed (Fig. 1E). On the other hand, we have shown that reproductive heteroblasty is affected by temperature (Fig. 5A–C). Our results indicate that changes in temperature, which are probably perceived at the fruit level (Supplementary Fig. S6), modulate the impact of age on fruit and seed production.

Ultimately, our data suggest that the combined perception of parental age and temperature is integrated to control the development of inflorescences and offspring seeds. Although the molecular basis for this integration remains to be formally addressed, recent research has revealed novel roles for flowering time genes in the control of seed size (Zhang *et al.*, 2020; Yu *et al.*, 2023). Here, we have focused on the floral integrator *FT*, which we previously identified as a regulator of arrest (González-Suárez *et al.*, 2023) and whose expression in fruits can affect seed germination (Chen *et al.*, 2014; Liu *et al.*, 2014). We have demonstrated that *FT* is necessary for the response to temperature and age during inflorescence development (Figs 5D–F, 6A, B), as well as for the integration of said cues at the level of seed germination (Fig. 6C, D). We have established that *FT* expression in the fruits is temperature sensitive, similar to other plant tissues (Blázquez *et al.*, 2003; Thines *et al.*, 2014). While expression of *FT* in fruits has been previously reported (Chen *et al.*, 2014), our results suggest that only the youngest, developing fruits express *FT* (Fig. 6E), suggesting that *FT*-dependent control over fruit and seed traits takes place early in fruit and seed development. The *FT* homologue *TERMINAL FLOWER 1* (*TFL1*) affects seed size through a well-described pathway that affects the cellularization of the endosperm (Zhang *et al.*, 2020). *TFL1* and *FT* tend to have antagonistic roles during development, and they can compete for the transcriptional regulation of the same target genes (Zhang *et al.*, 2020), raising the possibility that *FT* controls seed traits by acting through the same pathway. However, more detailed analysis of *FT* expression in dissected fruits and seeds would be needed to test this idea.

Our results have clear implications for understanding the effects of rising global temperatures on reproductive development of plants. While the effects of increased temperatures on male fertility in plants are well described (Hatfield and Prueger, 2015; De Storme and Geelen, 2020), our results demonstrate that increased temperatures also directly affect the size, seed number, and seed area of developing fruits, and the natural heteroblastic development of inflorescences. Thus, there are multiple intersecting mechanisms by which temperature will decrease global yields of fruit and seed crops. However, our results also show that these effects arise through modulation of FT expression during fruit development, and therefore can also potentially be mitigated by preventing excessive FT transcription in warmer temperatures. Our work thus provides a framework for defining the role of FT in inflorescence heteroblasty, although more research will be required to pin-point FT's exact role in control of fruit and seed development.

## Supplementary data

The following supplementary data are available at [JXB online](#).

Table S1. Primer sequences used for RT-qPCR.

Table S2. ANOVA for the linear models fitted in Fig. 5.

Table S3. Summary of predictors for the linear models fitted in Fig. 5.

Table S4. ANOVA for the linear models fitted in Fig. 6.

Table S5. Summary of predictors for the linear models fitted in Fig. 6.

Fig. S1. Heteroblastic changes in internode length along the inflorescence.

Fig. S2. Inflorescence arrest phenotypes of the *A. thaliana* accessions used.

Fig. S3. Flowering and end of flowering traits of plants from different deciles.

Fig. S4. Meristem diameter, fruit length, and internode length during flowering.

Fig. S5. Relationship between fruit length and seed number per fruit.

Fig. S6. Temperature experienced during fruit development affects heteroblasty.

Fig. S7. FT expression in the fruits is up-regulated at higher temperature.

## Acknowledgements

We thank Roza Bilas for technical assistance during plant growth experiments, and Amanda Bretman for feedback and analytical help during the preparation of this manuscript.

## Author contributions

TB, PG-S, and CHW: design; PG-S, CHW, and TL: performing experiments. PG-S: writing with inputs from other authors. All the authors

contributed to the data analysis and discussion, and reviewed and revised the manuscript.

## Conflict of interest

The authors declare that they have no conflict of interest.

## Funding

TB and CHW are supported by BBSRC grant BB/X001423/1. CHW was supported by a BBSRC White Rose PhD studentship (BB/M011151/1). PGS was supported by a studentship from the Faculty of Biological Science, Leeds.

## Data availability

All figures in this manuscript are associated with raw data. All data will be made available upon request.

## References

- Allsopp A. 1967. Heteroblastic development in vascular plants. *Advances in Morphogenesis* **6**, 127–171.
- Balanà V, Martínez-Fernández I, Sato S, Yanofsky MF, Kaufmann K, Angenent GC, Bemer M, Ferrándiz C. 2018. Genetic control of meristem arrest and life span in *Arabidopsis* by a FRUITFULL–APETALA2 pathway. *Nature Communications* **9**, 565.
- Bangerth F. 1989. Dominance among fruits/sinks and the search for a correlative signal. *Physiologia Plantarum* **76**, 608–614.
- Barks PM, Laird RA. 2015. Senescence in duckweed: age-related declines in survival, reproduction and offspring quality. *Functional Ecology* **29**, 540–548.
- Blázquez MA, Ahn JH, Weigel D. 2003. A thermosensory pathway controlling flowering time in *Arabidopsis thaliana*. *Nature Genetics* **33**, 168–171.
- Cartolano M, Pieper B, Lempe J, Tattersall A, Huijser P, Tresch A, Darrah PR, Hay A, Tsiantis M. 2015. Heterochrony underpins natural variation in *Cardamine hirsuta* leaf form. *Proceedings of the National Academy of Sciences, USA* **112**, 10539–10544.
- Chen M, MacGregor DR, Dave A, Florance H, Moore K, Paszkiewicz K, Smirnov N, Graham IA, Penfield S. 2014. Maternal temperature history activates flowering locus T in fruits to control progeny dormancy according to time of year. *Proceedings of the National Academy of Sciences, USA* **111**, 18787–18792.
- Chmilar SL, Laird RA. 2023. Effects of parental age on salt stress tolerance in an aquatic plant. *Oikos* **2023**, e09218.
- De Storme N, Geelen D. 2020. High temperatures alter cross-over distribution and induce male meiotic restitution in *Arabidopsis thaliana*. *Communications Biology* **3**, 187.
- Dogra H, Dani KGS. 2019. Defining features of age-specific fertility and seed quality in senescing indeterminate annuals. *American Journal of Botany* **106**, 604–610.
- Gomez MD, Barro-Trastoy D, Escoms E, *et al.* 2018. Gibberellins negatively modulate ovule number in plants. *Development* **145**, dev163865.
- González-Suárez P, Walker CH, Bennett T. 2023. FLOWERING LOCUS T mediates photo-thermal timing of inflorescence meristem arrest in *Arabidopsis thaliana*. *Plant Physiology* **192**, 2276–2289.
- Hatfield JL, Prueger JH. 2015. Temperature extremes: effect on plant growth and development. *Weather and Climate Extremes* **10**, 4–10.

- Hensel LL, Grbic V, Baumgarten DA, Bleecker AB.** 1993. Developmental and age-related processes that influence the longevity and senescence of photosynthetic tissues in *Arabidopsis*. *The Plant Cell* **5**, 553–564.
- House C, Roth C, Hunt J, Kover PX.** 2010. Paternal effects in *Arabidopsis* indicate that offspring can influence their own size. *Proceedings of the Royal Society B: Biological Sciences* **277**, 2885–2893.
- Koornneef M, Hanhart CJ, van der Veen JH.** 1991. A genetic and physiological analysis of late flowering mutants in *Arabidopsis thaliana*. *Molecular & General Genetics* **229**, 57–66.
- Krannitz PG, Aarssen LW, Dow JM.** 1991. The effect of genetically based differences in seed size on seedling survival in *Arabidopsis thaliana* (Brassicaceae). *American Journal of Botany* **78**, 446–450.
- Krzyszton M, Sacharowski SP, Manjunath VH, Muter K, Bokota G, Wang C, Plewczyński D, Dobisova T, Swiezewski S.** 2023. Dormancy heterogeneity among *Arabidopsis thaliana* seeds is linked to individual seed size. *Plant Communications* **5**, 100732.
- Landrein B, Refahi Y, Besnard F, Hervieux N, Mirabet V, Boudaoud A, Vernoux T, Hamant O.** 2015. Meristem size contributes to the robustness of phyllotaxis in *Arabidopsis*. *Journal of Experimental Botany* **66**, 1317–1324.
- Lenser T, Tarkowská D, Novák O, Wilhelmsson PKI, Bennett T, Rensing SA, Strnad M, Theißen G.** 2018. When the BRANCHED network bears fruit: how carpel dominance causes fruit dimorphism in *Aethionema*. *The Plant Journal* **94**, 352–371.
- Liu C, Thong Z, Yu H.** 2009. Coming into bloom: the specification of floral meristems. *Development* **136**, 3379–3391.
- Liu L, Farrona S, Klemme S, Turck FK.** 2014. Post-fertilization expression of FLOWERING LOCUS T suppresses reproductive reversion. *Frontiers in Plant Science* **5**, 164.
- Manning P, Houston K, Evans T.** 2009. Shifts in seed size across experimental nitrogen enrichment and plant density gradients. *Basic and Applied Ecology* **10**, 300–308.
- Merelo P, González-Cuadra I, Ferrándiz C.** 2022. A cellular analysis of meristem activity at the end of flowering points to cytokinin as a major regulator of proliferative arrest in *Arabidopsis*. *Current Biology* **32**, 749–762.e3.
- Murali KS.** 1997. Patterns of seed size, germination and seed viability of tropical tree species in Southern India. *Biotropica* **29**, 271–279.
- Pardos M, Vázquez-Piqué J, Benito L, Madrigal G, Alejano R, Fernández M, Calama R.** 2022. Does the age of *Pinus sylvestris* mother trees influence reproductive capacity and offspring seedling survival? *Forests* **13**, 937.
- Pidkowich MS, Klenz JE, Haughn GW.** 1999. The making of a flower: control of floral meristem identity in *Arabidopsis*. *Trends in Plant Science* **4**, 64–70.
- Quiroz S, Yustis JC, Chávez-Hernández EC, Martínez T, Sanchez M de la P, Garay-Arroyo A, Álvarez-Buylla ER, García-Ponce B.** 2021. Beyond the genetic pathways, flowering regulation complexity in *Arabidopsis thaliana*. *International Journal of Molecular Sciences* **22**, 5716.
- Robson JK, Tidy AC, Thomas SG, Wilson ZA.** 2023. Environmental regulation of male fertility is mediated through *Arabidopsis* transcription factors bHLH89, 91, and 10. *Journal of Experimental Botany* doi: [10.1093/jxb/erac480](https://doi.org/10.1093/jxb/erac480).
- Schmidt J, Claussen J, Wörlein N, Eggert A, Fleury D, Garnett T, Gerth S.** 2020. Drought and heat stress tolerance screening in wheat using computed tomography. *Plant Methods* **16**, 15.
- Schneider CA, Rasband WS, Eliceiri KW.** 2012. NIH Image to ImageJ: 25 years of image analysis. *Nature Methods* **9**, 671–675.
- Shapiro SS, Wilk MB.** 1965. An analysis of variance test for normality (complete samples). *Biometrika* **52**, 591–611.
- Thines BC, Youn Y, Duarte MI, Harmon FG.** 2014. The time of day effects of warm temperature on flowering time involve PIF4 and PIF5. *Journal of Experimental Botany* **65**, 1141–1151.
- Tsukaya H, Shoda K, Kim G-T, Uchimiya H.** 2000. Heteroblasty in *Arabidopsis thaliana* (L.) Heynh. *Planta* **210**, 536–542.
- van Mólken T, Jorritsma-Wienk LD, van Hoek PHW, de Kroon H.** 2005. Only seed size matters for germination in different populations of the dimorphic *Tragopogon pratensis* subsp. *pratensis* (Asteraceae). *American Journal of Botany* **92**, 432–437.
- Walker CH, Ware A, Šimura J, Ljung K, Wilson Z, Bennett T.** 2023. Cytokinin signaling regulates two-stage inflorescence arrest in *Arabidopsis*. *Plant Physiology* **191**, 479–495.
- Walker CH, Wheeldon CD, Bennett T.** 2021. Integrated dominance mechanisms regulate reproductive architecture in *Arabidopsis thaliana* and *Brassica napus*. *Plant Physiology* **186**, 1985–2002.
- Wang J-W.** 2014. Regulation of flowering time by the miR156-mediated age pathway. *Journal of Experimental Botany* **65**, 4723–4730.
- Wang L, Zhou C-M, Mai Y-X, et al.** 2019. A spatiotemporally regulated transcriptional complex underlies heteroblastic development of leaf hairs in *Arabidopsis thaliana*. *The EMBO Journal* **38**, e100063.
- Wang Y, Kumaishi K, Suzuki T, Ichihashi Y, Yamaguchi N, Shirakawa M, Ito T.** 2020. Morphological and physiological framework underlying plant longevity in *Arabidopsis thaliana*. *Frontiers in Plant Science* **11**, 1693.
- Ware A, Walker CH, Šimura J, González-Suárez P, Ljung K, Bishopp A, Wilson ZA, Bennett T.** 2020. Auxin export from proximal fruits drives arrest in temporally competent inflorescences. *Nature Plants* **6**, 699–707.
- Westoby M, Leishman M, Lord J.** 1997. Comparative ecology of seed size and dispersal. *Philosophical Transactions of the Royal Society B: Biological Sciences* **351**, 1309–1318.
- Wuest SE, Philipp MA, Guthörl D, Schmid B, Grossniklaus U.** 2016. Seed production affects maternal growth and senescence in *Arabidopsis*. *Plant Physiology* **171**, 392–404.
- Yoo SK, Chung KS, Kim J, Lee JH, Hong SM, Yoo SJ, Yoo SY, Lee JS, Ahn JH.** 2005. CONSTANS activates SUPPRESSOR OF OVEREXPRESSION OF CONSTANS 1 through FLOWERING LOCUS T to promote flowering in *Arabidopsis*. *Plant Physiology* **139**, 770–778.
- Yu B, He X, Tang Y, et al.** 2023. Photoperiod controls plant seed size in a CONSTANS-dependent manner. *Nature Plants* **9**, 343–354.
- Yuan J, Kessler SA.** 2019. A genome-wide association study reveals a novel regulator of ovule number and fertility in *Arabidopsis thaliana*. *PLoS Genetics* **15**, e1007934.
- Zhang B, Li C, Li Y, Yu H.** 2020. Mobile TERMINAL FLOWER1 determines seed size in *Arabidopsis*. *Nature Plants* **6**, 1146–1157.